Cooling the Tip of a Turbine Blade Using Pressure Side Holes—Part II: Heat Transfer Measurements

J. R. Christophel

K. A. Thole

Mechanical Engineering Department,
Virginia Polytechnic Institute and State University,
Blacksburg, VA 24061

F. J. Cunha

Pratt & Whitney,
United Technologies Corporation,
East Hartford, CT 06108

The clearance gap between a turbine blade tip and its associated shroud allows leakage flow across the tip from the pressure side to the suction side of the blade. Understanding how this leakage flow affects heat transfer is critical in extending the durability of a blade tip, which is subjected to effects of oxidation and erosion. This paper is the second of a two-part series that discusses the augmentation of tip heat transfer coefficients as a result of blowing from film-cooling holes placed along the pressure side of a blade and from dirt purge holes placed on the tip. For the experimental investigation, three scaled-up blades were used to form a two-passage, linear cascade in a low-speed wind tunnel. The rig was designed to simulate different tip gap sizes and film-coolant flow rates. Heat transfer coefficients were quantified by using a constant heat flux surface placed along the blade tip. Results indicate that increased film-coolant injection leads to increased augmentation levels of tip heat transfer coefficients, particularly at the entrance region to the gap. Despite increased heat transfer coefficients, an overall net heat flux reduction to the blade tip results from pressure-side cooling because of the increased adiabatic effectiveness levels. The area-averaged results of the net heat flux reduction for the tip indicate that there is (i) little dependence on coolant flows and (ii) more cooling benefit for a small tip gap relative to that of a large tip gap. [DOI: 10.1115/1.1811096]

Introduction

Technical advancements in the gas turbine industry require higher turbine rotor inlet temperatures to allow for more efficient operation and engine performance. Inlet temperatures to the rotor are, however, the limiting design criteria because these temperatures, in turn, decrease component life for the same material and cooling technology. Gas turbine airfoils are typically cooled using both convective and film cooling. Film cooling is a method whereby cooler compressor fluid is injected through film holes in the blade surface. This type of protection is important for a turbine blade tip where the heat transfer coefficients can be over two times greater than those on the pressure side of the blade [1]. As such, film-cooling holes can be placed on the pressure side of a turbine blade near the tip region. Because of the pressure-driven flow over the tip, the coolant from these holes sweeps over the tip through the gap clearance thereby providing coolant along the blade tip.

The purpose of this study was twofold. The first part examined the heat transfer on a flat blade tip without cooling to verify fundamental trends. The second part examined the heat transfer coefficients for two different tip gap settings and a range of coolant flows for blowing through combined pressure-side and dirt purge holes. The results from this study were combined with adiabatic effectiveness results from Part I [2] to evaluate the overall benefit of the tip cooling.

Past Relevant Studies

As early as 1982, Mayle and Metzger [3] showed that the tip leakage flow is composed primarily of mainstream passage fluid. Other researchers showed a separation bubble formation along the tip pressure side, which was confirmed by Morphis and Bindon [4]. Bindon [5] went on to show that this separation bubble dominates the gap flow characteristics and associated pressure losses. In his recent review of turbine blade tip heat transfer, Bunker [6] noted that this separation bubble causes a heat transfer enhancement factor of two to three times above that occurring at the tip camber line of an airfoil.

In an effort to reduce the tip leakage flow, many studies have been performed on blade tips with a squealer geometry. This geometry has been shown to significantly reduce the blade tip heat transfer; however, the trends seen on a flat tip are much different from a tip with a squealer cavity. Bunker et al. [7], using a recessed shroud, showed the first experimental heat transfer results on a flat blade tip. His research showed there to be a small area of low heat transfer located near the thickest part of the blade. This low region has been confirmed by many authors, including Kwak and Han [1] and Jin and Goldstein [8]. Kwak and Han [1] also noted that the area of low heat transfer tends to be smaller and pushed downstream at increased gaps.

Azad et al. [9], Teng et al. [10], Kwak and Han [11], and Jin and Goldstein [8] have all shown that the blade tip heat transfer increases with increasing tip gap height. This increase can be explained by the fact that larger gap heights reduce the path length to hydraulic diameter ratio (L/D_h), thereby causing more of the tip surface to be affected by the entry region effects for larger gap heights. For a flat tip with no blowing, Jin and Goldstein [8] showed that the average heat transfer increases along the blade toward the trailing edge. This increase was confirmed by Saxena et al. [12] who showed that the heat transfer along the blade camber line increased toward the trailing edge. One of the recent computational studies by Ameri [13] indicated that a sharp edge along the pressure side (with no blowing) was more effective in reducing the tip leakage flow relative to a rounded edge.

There have been relatively few studies with blowing over a blade tip surface. Kim and Metzger [14] and Kim et al. [15] measured the heat transfer coefficients along a channel representing a blade tip with various film-cooling injection geometries. They showed that injection always led to increases in heat transfer over no injection over most of their surface simulating a blade tip (except their round hole injection, which showed no change). Kwak and Han [11] used an airfoil shape with both tip and pressure-side

Contributed by the International Gas Turbine Institute (IGTI) of THE AMERICAN SOCIETY OF MECHANICAL ENGINEERS for publication in the ASME JOURNAL OF TURBOMACHINERY. Paper presented at the International Gas Turbine and Aeroengine Congress and Exhibition, Vienna, Austria, June 13–17, 2004, Paper No. 2004-GT-53254. Manuscript received by IGTI, October 1, 2003; final revision, March 1, 2004. IGTI Review Chair: A. J. Strazisar.

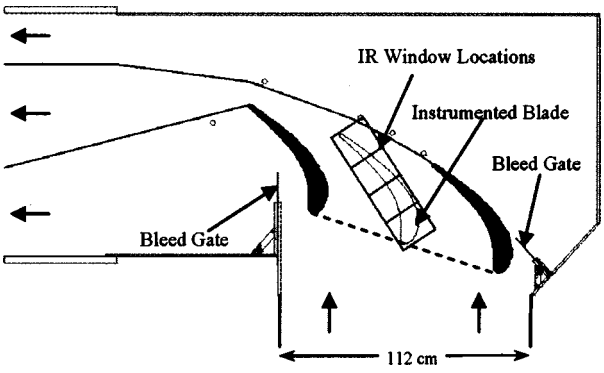

Fig. 1 Test section viewed from top showing adjustment capabilities and infrared windows

injection. Their results indicated a decrease in heat transfer coefficients with increased blowing between the pressure-side edge and camber line.

Generally, tip heat transfer studies without injection have all shown that increasing the tip gap increases heat transfer. Also, regions of low heat transfer are expected near the thickest portions of the blade. When coolant injection is introduced, however, the results are still unclear. This study will assess the effects of blowing ratio and tip gap height on tip heat transfer when blowing is present near the pressure-side tip combined with dirt purge holes.

Experimental Facility and Instrumentation

The experiments in this study were performed in a large-scale, low-speed, closed-loop wind-tunnel facility that provided matched-engine Reynolds number conditions, as described in Part 1 [2]. The test section was attached downstream of a contraction section that used a row of high-momentum normal jets to provide a turbulence level of 10% and length scale of 11 cm at the blade entrance. The linear cascade test section, shown in Fig. 1, consisted of an instrumented center blade and two outer blades with tailboards. The tailboards and the bleed gates allowed for flow control around the center blade, insuring flow periodicity. Static pressure measurements were taken at the blade midspan to ensure flow periodicity.

Coolant flow used for the tip-blowing experiments was supplied by an in-house compressor and was controlled by using a series of valves before exiting through the blade tip cooling holes. The overall coolant flow rate was known by measuring the pressure drop across a venturi nozzle. Discharge coefficients, which had previously been measured, allowed for the estimation of flow rate through each individual hole by way of pressure measurements [2]. The total coolant flow could then be calculated by summing each of the individual flows. This calculation for each hole was summed and compared to the total coolant flow measured by the venturi nozzle. In general, the two flows were within 2.8%. The two tips that were tested, shown in Fig. 2, are referred to as the baseline (Fig. 2(*a*)) and cooling hole (Figs. 2(*b*) and 2(*c*)) models. Both blades had a dirt purge cavity that was recessed 2h (0.67H) from the tip surface. The baseline geometry had no holes present on the pressure side or within the dirt purge cavity and, therefore, no film cooling. The cooling-hole model had tip holes placed on the pressure-side surface of the blade in addition to two holes within the dirt purge cavity, which have been described in detail by Hohlfeld et al. [16]. The purpose of the dirt purge holes is to allow for blade manufacturing and to expel dirt particles so as not to plug smaller diameter film-cooling holes.

In addition to the dirt purge holes, the four film-cooling holes just downstream of the stagnation were expanded in the axial direction and had a metering hole diameter of 0.56 D whereas the remainder of the holes had no expansion and a metering hole

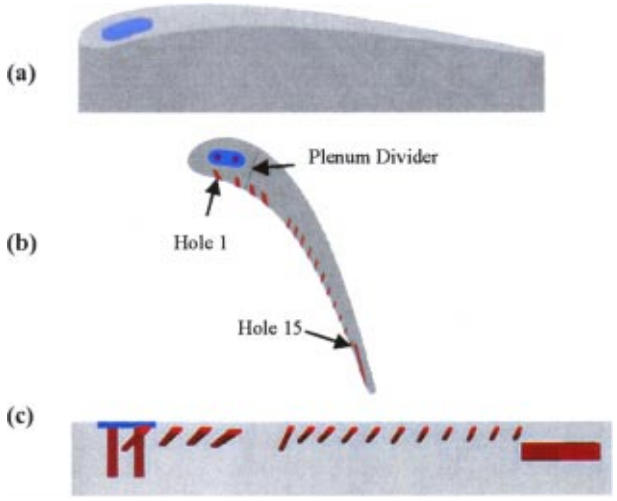

Fig. 2 Tip geometries tested: (*a*) the baseline geometry (filled-in dirt purge holes) and (*b*),(*c*) approximate hole geometry with the dirt purge holes

diameter of 0.41 D. The tip model also contained a slot at the trailing edge denoted as the trailing edge flag (TEF).

Testing conditions and blade parameters are given in Table 1. The small h and large H tip gap settings considered were 0.54% and 1.63% of full blade span, respectively. All heat transfer coefficient tests were conducted at a density ratio of one, such that the coolant and mainstream temperatures were kept to within 0.15°C. For the baseline geometry, experiments were conducted at both the small and large tip gap settings with no blowing present. For the cooling-hole geometry, experiments were conducted at both tip gap settings and at overall coolant flow rates of 0.58% and 1% of the total passage flow. The total passage flow was calculated based on the inlet mainstream velocity, blade span, and pitch. The local blowing ratios are reported in Part I [2].

For making the heat transfer measurements, foil heaters were used to supply a constant heat flux at the tip surface. Two separate heaters were necessary that included one for the blade tip surface and the other for the dirt purge cavity on the tip. The dirt purge cavity was heated with one strip of Inconel that was 0.051 mm thick and had a surface area of 17.3 cm^2. The main heater covered an area of 261.2 cm^2 and consisted of a serpentine Inconel circuit. The circuit, shown in Fig. 3, used Inconel sandwiched between insulating Kapton and then covered with a very thin (0.013 mm) layer of copper on both sides. Both heaters were attached to a foam blade tip using double-sided tape that was 0.64 mm thick. The nominal heat flux for both heaters was set to 3700 W/m^2, which provided a maximum temperature difference between the mainstream and blade surface of 28°C. The two heaters were controlled independently with a variac to within 0.67% of one an-

Table 1 Testing Conditions and Blade Parameters

Parameter	Wind tunnel settings
Scaling Factor	12×
Axial chord/true chord	0.66
Pitch/true chord	0.81
Span/true chord	1.03
Re_{in}	2.1×10^5
Inlet angle, θ	16.5 deg
T_∞(°C)	21
Small tip gap/span (%)	0.54
Large tip gap/span (%)	1.63

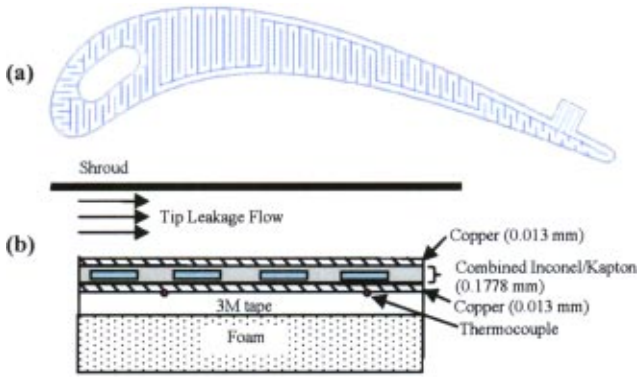

Fig. 3 Main tip heat transfer surface showing (*a*) serpentine passages and (*b*) detail of main tip heater as placed on the blade surface

other during all tests. The current supplied to each heater was known by placing a precision resistor ($R=1\Omega\pm0.1\%$) in each circuit and measuring the voltage drop across each resistor with a digital multimeter. The heater power was then determined from the supplied current and known heater resistance.

Equation (1) was used when calculating the heat transfer results to account for radiation losses,

$$h=(q''_{\text{tot}}-q''_r)/(T_w-T_\infty) \tag{1}$$

In this equation, q''_{tot} represents the total heat flux output from the resistive heaters and q''_r represents the energy lost to radiation. Typically, radiation losses were less than 2% with the maximum for all cases being 3.4%. Conduction losses were found to be negligible because the heaters were placed on low-thermal-conductivity foam.

The surface temperatures on the tip (T_w) were obtained using an Inframetrics P20 infrared (IR) camera. The images were processed with Thermacam Researcher 2002® and using an in-house MATLAB code. Four IR images were acquired through the zinc selenide windows placed in the shroud surface to cover the entire blade, as shown in Fig. 1. Each image covered an area that was 21.3 cm by 16 cm and contained 320 by 240 pixels. The camera was located approximately 55 cm from the tip, resulting in a spatial resolution of 0.63 mm. For every test, each of the four images was taken five times, and the average of these five images was used.

Each image was calibrated using thermocouples placed underneath the heater. These thermocouples were held in place with a highly thermal conductive adhesive ($k=1.6$ W/mK). This ensured that the thermocouple would read the surface temperature of the heater. This surface temperature was calculated to be 2°C less than the outer test copper surface for $q''=3700\,\text{W/m}^2$ due to the Kapton thermal resistance. This temperature difference was accounted for in the calibration process. The thermal resistance of the Inconel heater in the dirt purge cavity was found to be negligible, and no correction was needed for this area of the blade tip. The IR images were calibrated to a total of six thermocouples by adjusting the background temperature (T_b) and surface emissivity (ε). The emissivity is a surface property, which was set to 0.93 for all cases as a result of the heaters being painted with flat black paint. During the calibration process, all IR images were matched to the thermocouples to within 1.0°C. A check on the calibration process is that the four individual images matched up well to form one entire blade contour without any noticeable discontinuities in measured values between images.

Overall uncertainties were calculated for high and low values of heat transfer coefficients and Nusselt numbers according to the partial derivative method described in Moffat [17]. The total uncertainty of any measurement was calculated as the root of the sum of the squares of the precision and bias uncertainties. Based on a 95% confidence interval, the IR camera precision uncertainty was calculated to be 0.06°C. The manufacturers reported bias uncertainty is 2.0% full scale, where typical ranges were set to 20°C. The thermocouples used to determine mainstream and coolant temperatures had a reported bias uncertainty of ±0.2°C, and the precision uncertainty was determined to be ±0.1°C from repeated measurements. The total uncertainty in heat transfer measurements was 6% at $\text{Nu}_{Dh}=45$ and 10.5% at $\text{Nu}_{Dh}=55.7$.

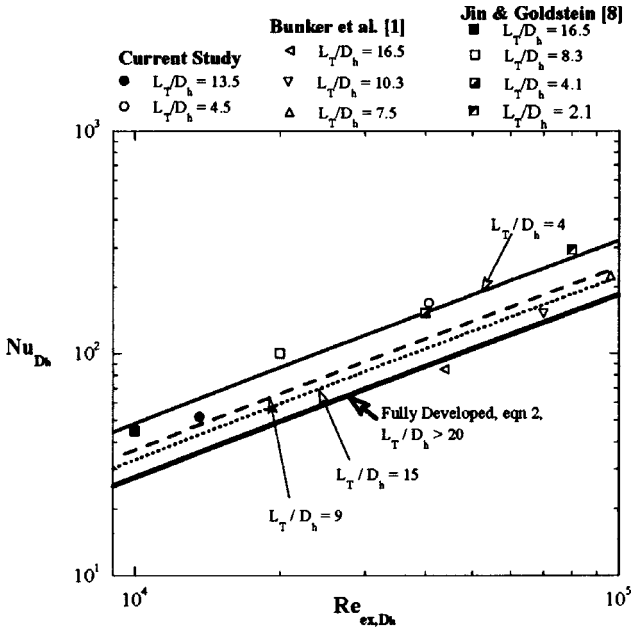

Fig. 4 Comparison of experimental data to a fully developed correlation

Tip Heat Transfer Coefficients

Previous studies have compared flow in a turbine blade tip gap region to that of a fully developed channel flow correlation for turbulent flow in a duct. The correlation that was used for comparison in our paper was developed by Gnielinski [18]. Gnielinski's correlation is given in Eq. (2) and has been reported in the literature to provide accuracy to within 6% as reported by Kakaç et al. [19] for a large Reynolds number range ($10^4<\text{Re}<10^6$).

$$\text{Nu}_{fd}=hD_h/k=0.0214(\text{Re}^{0.8}-100)\text{Pr}^{0.4} \tag{2}$$

Mayle and Metzger [3] furthered this correlation for a tip gap by adding an augmentation factor to account for the overwhelming entry region effects of thin blade tips. This augmentation factor, which was taken from Kays and Crawford [20], allows blade designers to relate overall blade tip heat transfer (for a given blade thickness and tip gap) to an overall heat transfer expected in a fully developed channel. Using data collected in this study, comparisons have been made to the data of Jin and Goldstein [8] and Bunker et al. [7] that confirm this augmentation factor approach. Although Mayle and Metzger [3] first noted the augmentation factor, their data have not been included in this comparison because only experiments performed on airfoil shapes were considered.

Figure 4 shows Nusselt number values based on the hydraulic diameter of the tip gap (2h or 2H) plotted as a function of the blade Reynolds number based on the exit velocity and hydraulic diameter. The Gnielinski correlation has been plotted for several L_T/D_h ratios as shown on the plot. Note that L_T represents the maximum thickness of the blade. As known for the turbulent channel flow, fully developed conditions generally occur for $L/D_h>20$ [20]. There is fairly good agreement between experi-

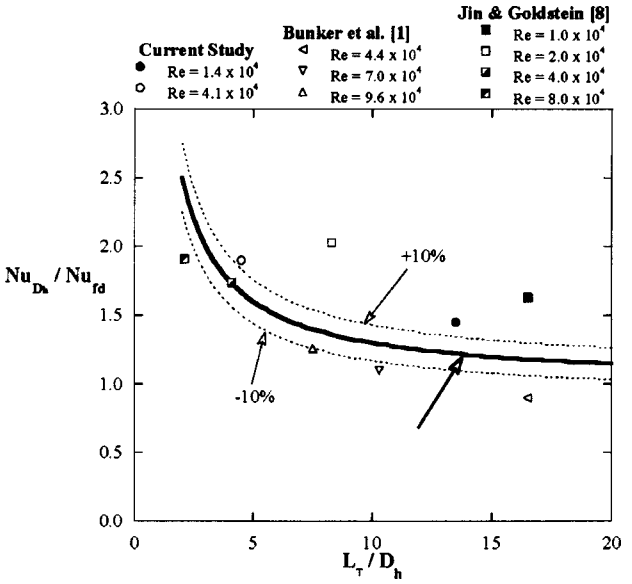

Fig. 5 Comparison of experimental data to the proposed augmentation factor

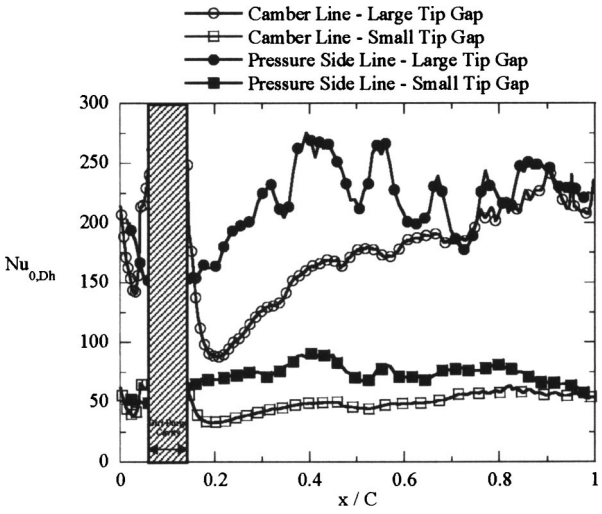

Fig. 7 Nusselt number line plots for the baseline

mental data and the appropriate correlations. It should be noted that the L_T/D_h ratios are based on the maximum blade thickness, and the Nusselt numbers are the average values calculated for the tip surface. Therefore, this ratio is not a perfect representation of a blade profile, but works reasonably well for the area-averaged values shown here.

Figure 5 shows the same experimental data points, plotted as a ratio of the Nusselt number normalized by the fully developed correlation. The solid line represents the augmentation factor given by Kays and Crawford [20]. Most of the data points fall close to the line, with the exception of two Jin and Goldstein points: $\mathrm{Re}=1.0\times10^4$ and $\mathrm{Re}=2.0\times10^4$. These data points, however, are at low Reynolds numbers, which has been shown to greatly affect the heat transfer. Mayle and Metzger [3] showed that low Reynolds numbers can cause an increase of 20–30% above of the expected augmentation factors used in Fig. 5. More experiments should be performed to further verify this trend.

Baseline Results (No Blowing). The baseline results with no blowing are presented as contour plots of Nusselt number in Fig. 6. Note that the chord rather than hydraulic diameter was used for these contour plots to illustrate the differences in the heat transfer coefficients along the blade tip for both tip gaps. Results at both gap heights show similar trends, however. The large tip gap shows

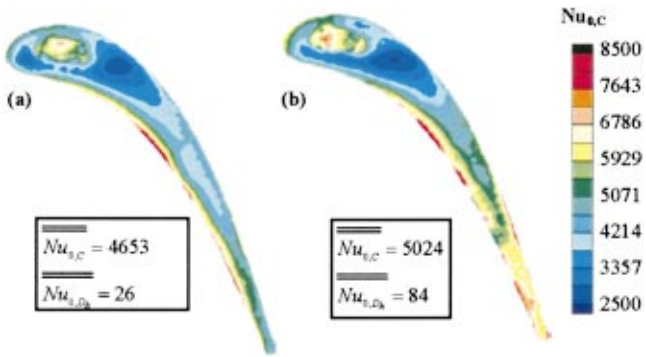

Fig. 6 Baseline Nusselt number contour plots for the (*a*) small and (*b*) large tip gap

higher Nusselt numbers at the blade trailing edge relative to the small tip gap. This increase in heat transfer at the larger tip gap trailing edge is a result of the increased entry region effect relative to the small tip gap. With smaller L/D_h values (for the large tip gap), the entry region is expected to have a greater effect, as mentioned at the beginning of this section. For the large tip gap, the L/D_h is as low as 1 across the trailing edge of the tip surface, whereas for the small tip gap, the L/D_h is 3.5.

The area-averaged Nusselt numbers are given for each case to quantify the increase in heat transfer with gap height. For these cases, the Nusselt number at the large tip gap is 3.2 times that of the small tip gap when based on the exit velocity and hydraulic diameter. By using Reynolds number scaling, the large tip gap is expected to have 2.4 times the heat transfer of the small tip gap. This larger-than-expected increase results from the overwhelming entry-region effect, which serves to greatly increase tip heat transfer coefficients.

As shown in Fig. 6, there are regions of low heat transfer immediately downstream of the dirt purge cavity for both tip gap heights. This is near the thickest portion of the blade and represents the area of lowest heat transfer on the blade tip. This region was first pointed out by Bunker [6] and has been confirmed by other authors. Within the dirt purge cavity, there are high heat transfer coefficients resulting from low velocity flow recirculation in the cavity. Overall, the leading-edge region experiences relatively low heat transfer outside of the dirt purge cavity in comparison to the trailing edge.

Also seen on these contour plots are regions of high heat transfer coefficients along the pressure side that begin around the leading edge at $S/S_{\max}=0.1$ and extend until the trailing edge. These regions of high heat transfer have been noted by Morphis and Bindon [4], Bindon [5], and Teng et al. [10] to be the separation region that forms along the pressure side due to mainstream and leakage flow interaction. This region occurs within the entry region and is more dominant at the large tip gap than at the small tip gap, and extends over a large region of the tip for the large tip gap. To further study the effects of this entry region, line plots have been made that compare Nusselt numbers at the pressure side of the tip to those of the blade camber line in Fig. 7. Note that Nusselt numbers displayed from this point forward in the paper are given based on the hydraulic diameter D_h. Shown in Fig. 7, these line plots show similar trends at both tip gaps.

For the blade camber line data shown in Fig. 7, there are very low values for both tip gaps immediately downstream of the dirt

Table 2 Positions for Line Plots

	Large tip gap		Small tip gap	
	Re_{Dh}	L/D_h	Re_{Dh}	L/D_h
Line 0	4.4×10^4	4.0	1.5×10^4	11.9
Line 1	4.7×10^4	4.0	1.6×10^4	12.1
Line 2	4.5×10^4	2.9	1.5×10^4	8.7
Line 3	4.4×10^4	2.7	1.5×10^4	8.1

purge cavity. Downstream of this area of low heat transfer, the camber line data increase as the blade becomes thinner. The pressure-side data begin to increase at about $x/C=0.15$ as the separation bubble begins to form. Nusselt numbers increase until $x/C=0.4$, where the maximum Nusselt numbers are reached for both tip gaps. Downstream of this location, the pressure-side data remain relatively constant with oscillating levels. These oscillations, seen especially at the large tip gap, suggest localized effects in the separation bubble most likely due to the sensitivity of the separation region to any imperfections at the corner of the blade tip. This separation region was also computationally predicted by Hohlfeld et al. [16]. At the very trailing edge of the blade, the camber and pressure-side lines become equal for the same gap height. This is because the tip is so thin that the entry region dominates the entire tip passage. In general, the pressure side of the blade tip experiences relatively high heat transfer and, as such, justifies the idea of adding pressure-side film-cooling holes.

To compare the baseline results to the turbulent channel flow correlation in Eq. (2), data have been taken along various lines across the tip. For each line to be compared to channel flow, the local inviscid velocity was used to calculate the Reynolds number. This velocity was found from the local pressure difference as predicted at the 95% blade span. The Reynolds number based on local velocity and D_h are given in Table 2 along with the L/D_h at each position. Line 0 is only of interest to the baseline cases because, when blowing is present, this area is affected by the dirt purge holes. Lines 1 and 2 were identified in Part 1 of this paper [2] as the locations having the maximum effectiveness levels while line 3 is between two jet trajectories. Figure 8 shows lines 0, at $S/S_{\max}=0.28$ for the baseline cases (no blowing). Note that for this plot, $L_{\max}$ is the maximum local blade thickness at each line location, and L is the distance along that line. Figure 8 shows that within the range of uncertainty, flow at both gap heights becomes fully developed at line 0. At line 3, the measured heat transfer is higher than the correlation. This is due to $L/D_h \leqslant 20$ at the trailing edge of the blade reflecting the influence of the entry region.

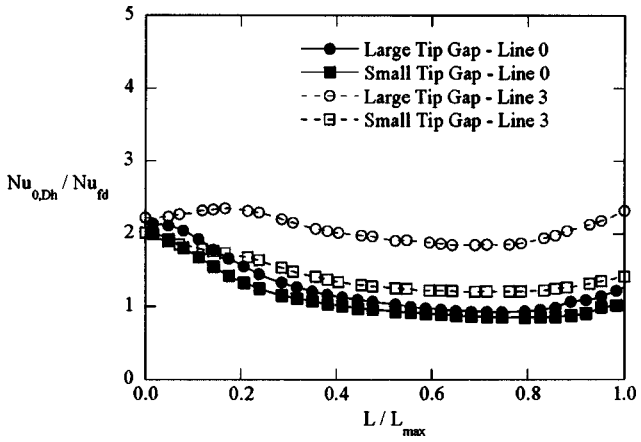

Fig. 8 Line plots at lines 0 and 3 for baseline cases

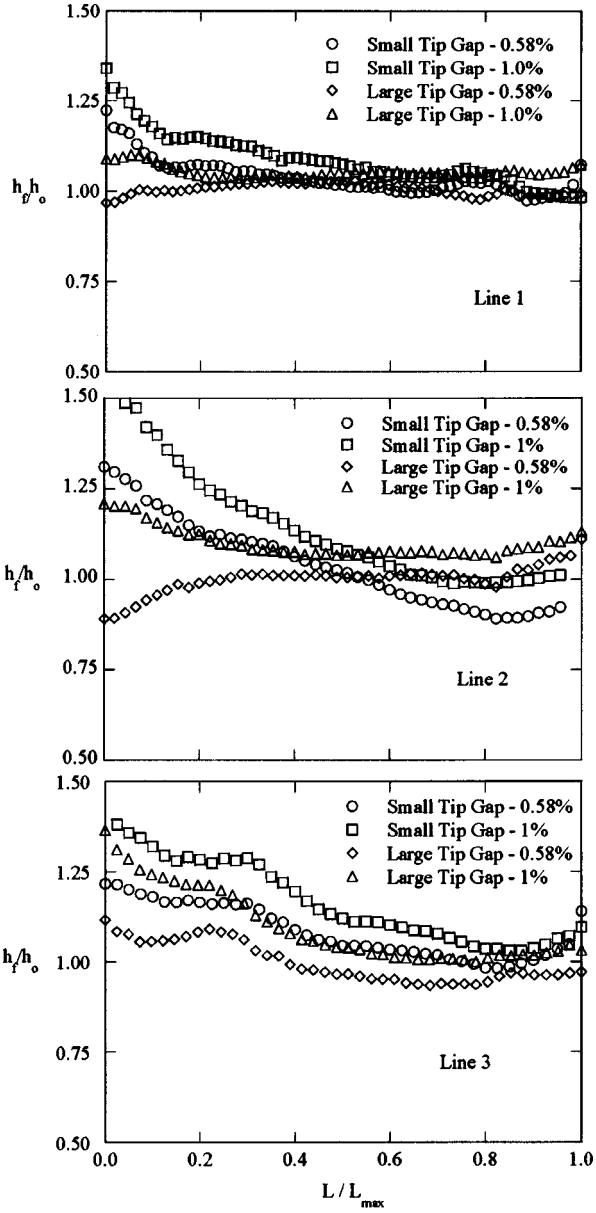

Fig. 9 (*a*)–(*c*) Line plots for the cooling holes at positions 1, 2, and 3

Film-Cooling Hole Results. The heat transfer measurements on the blade tip with blowing from pressure-side holes were compared to the baseline with no blowing. For this comparison, a h_f/h_0 ratio greater than one means that there is increased heat transfer with blowing, and a ratio less than one means that the heat transfer is reduced when blowing is present. Two lines were chosen to follow the peak effectiveness locations of separate film-cooling holes (lines 1 and 2), and a third line was chosen to follow in between two film-cooling holes (line 3).

Figures 9(*a*)–9(*c*) shows the comparison lines for the tip results with blowing. Blowing causes severe increases in heat transfer up to one hydraulic diameter into the large tip gap and up to five hydraulic diameters along the small tip gap. While the enhancement is not as pronounced for the remainder of the gap length, there is still an effect of blowing as h_f/h_0 values are generally above 1.

Based on the results shown in Figs. 9(*a*)–9(*c*) flow models can be described for the pressure side blowing. For the large tip gap, the flow separates from the blade pressure side and impinges upon

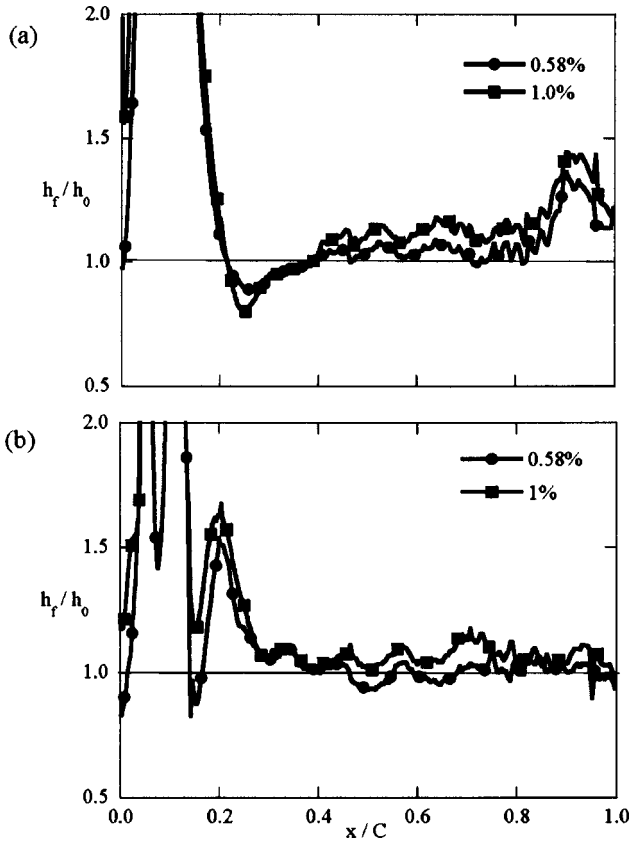

Fig. 10 Heat transfer augmentation at the camber line for the (*a*) small and (*b*) large tip gaps

the shroud. The separation region is enhanced by the high momentum flow from the holes thereby causing high augmentations of the heat transfer coefficients. For the small tip gap, the coolant jet fills in the separated region.

Data taken along the camber line are shown in Figs. 10(*a*)–(*b*) for the small and large tip gaps, respectively. Heat transfer augmentation within the dirt purge cavity is very high. Immediately after the dirt purge cavity between $0.2<x/C<0.3$, the large tip gap has a higher h_f/h_0 than the small tip gap. This is most likely due to vortices that are created by the dirt purge holes in the case of the large tip gap. Higher heat transfer augmentations occur on the downstream side of the second dirt purge hole, which is where

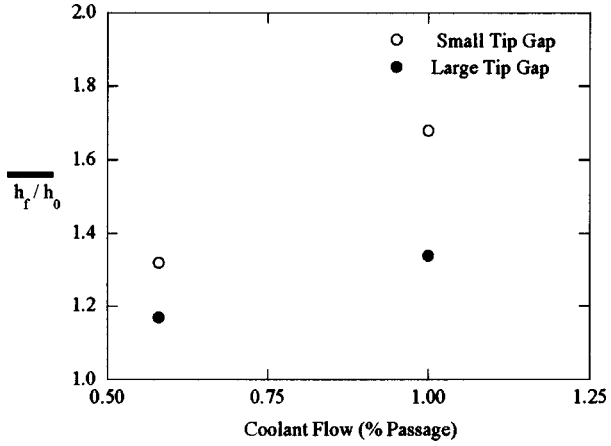

Fig. 11 Area-averaged heat transfer augmentation for the entire blade tip

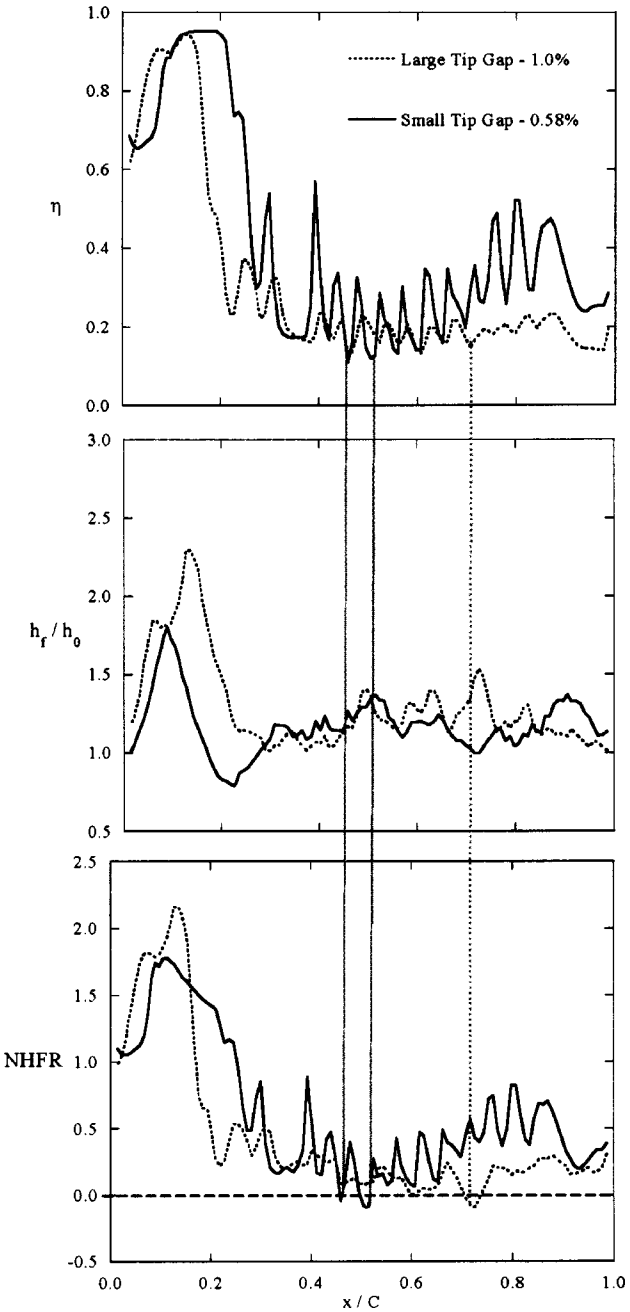

Fig. 12 Pressure side plots of NHFR for the small tip gap

the lowest heat transfer occurs for the baseline case. This combination results in high augmentation values at this location for the large gap.

At the small tip gap (Fig. 10(*a*)) augmentations decrease to below 1 around $x/C=0.2$. From $x/C=0.3$ to 1, the augmentations show a continued increase along the blade tip at the small tip gap. The increased heat transfer augmentation may likely be due to an increase in the size of the separation region along the pressure side of the tip. The results indicate that there is always an increase in the heat transfer augmentation with increased blowing. Kim et al. [15] showed that with a shaped hole, the heat transfer increases as much as 13% with a 60% increase in coolant flow. Results from this test show about an 8% increase in heat transfer for a 75% increase in coolant flow. The lower augmentations may be attributed to the compound injection angle and the cylindrical hole shape of these tests as compared to Kim et al.

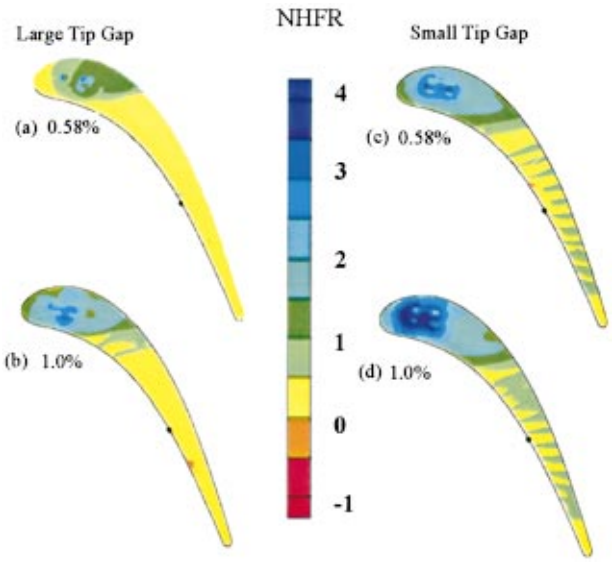

Fig. 13 NHFR for all cases at 0.58% and 1% coolant flow

For the large tip gap (Fig. 10(*b*)), the heat transfer ratio plot shows increased heat transfer augmentation with increased blowing. The area averages in Fig. 11 indicate the rise in the overall heat transfer coefficients as a result of blowing. There appears to be a larger difference between the small and large tip gaps at the higher coolant flow conditions. Overall augmentations for the small tip are larger than for the large tip gap at both blowing ratios.

Net Heat Flux Reduction. Combining the heat transfer measurements of this paper with the film effectiveness measurements of Part I [2], the overall cooling benefit is summarized in the net heat flux reduction (NHFR). Shown in Eq. (3), NHFR is an established method of evaluating the overall effect of a cooling scheme on a surface [21],

$$\mathrm{NHFR} = 1 - h_f/h_0(1 - \eta \cdot \theta) \tag{3}$$

In this equation, all variables have been measured experimentally except for θ. A constant value of 1.6, which corresponds to a cooling effectiveness of 62.5% (inverse of 1.6), was used for this paper and was based on the previous literature [21]. As this equation shows, when high heat transfer augmentation is not accompanied by high film cooling, the NHFR can become negative. A negative NHFR means that the cooling scheme is actually causing an increased heat load to the blade surface. Figure 12 shows two examples of an increased heat load for the small tip gap at 0.58% and for the large tip gap at 1% coolant flow. Line plots along the pressure side of the tip for η, h_f/h_0, and NHFR are shown. The vertical lines show the locations where NHFR is slightly negative. For the negative values relating to the small tip gap case, the negative NHFR comes from localized low values in η along with high heat transfer. These two locations are between film-cooling holes where the cooling effectiveness is low (because the cooling holes have relatively poor spreading) and heat transfer is high.

The NHFR values were calculated locally for each case and are shown in Fig. 13. Also shown in Fig. 13 is a location for one of the hole exits (black dot). Not all of the hole exits are shown for proprietary reasons. Generally the entire blade tip surface has positive values. Also, the leading edge tends to have high NHFR values resulting from the dirt purge blowing. There are noticeable streaks along the blade that are aligned with the film-cooling trajectories for the small tip gap.

To further study the NHFR along a cooling path, data were taken along the path lines described in Table 2. These results are shown in Fig. 14. Once again, lines 1 and 2 follow the direct path

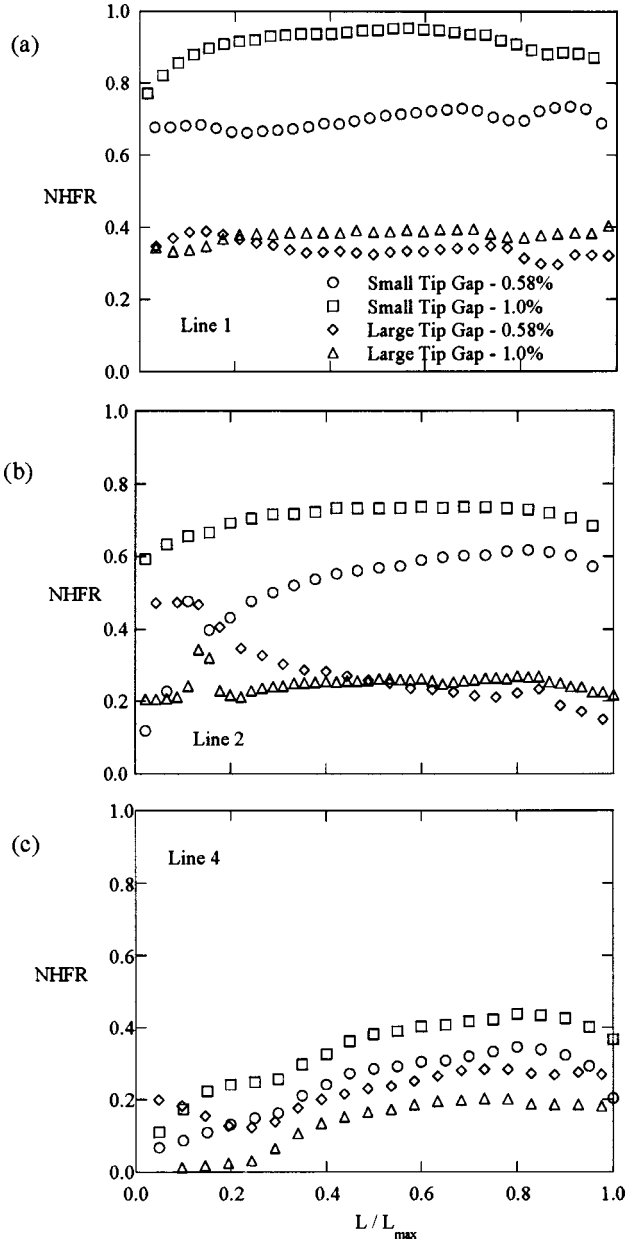

Fig. 14 (*a*)–(*c*) Individual line plots of NHFR at different locations along the blade tip

of coolant over the tip, and line 3 lies in between two coolant paths. Increased blowing levels result in increased NHFR values at the small tip gap, but not always at the large tip gap. As has been mentioned in Part 1, the lower coolant flow rates actually allow the jet paths to remain attached to the blade for the large tip gap. This is made evident at line 2. The 0.58% case starts off near NHFR=0.5 and quickly decreases as the low coolant flow is diffused with the main gap flow. For the 1% case, however, there is a constant NHFR ~0.2 across the entire gap width. This agrees with previous suggestions that the jets for the large tip gap separate from the blade and attach to the shroud at higher blowing rates. For line 3, which is in between two hole paths, similar results are seen as on the hole paths, such that at the small tip gap, increased blowing increases the NHFR, whereas at the large tip gap, the opposite is true.

NHFR results taken at the camber line are shown in Fig. 15. The results in Fig. 15(*a*) indicate much higher variation (meaning minimum to maximum differences) between hole locations at the

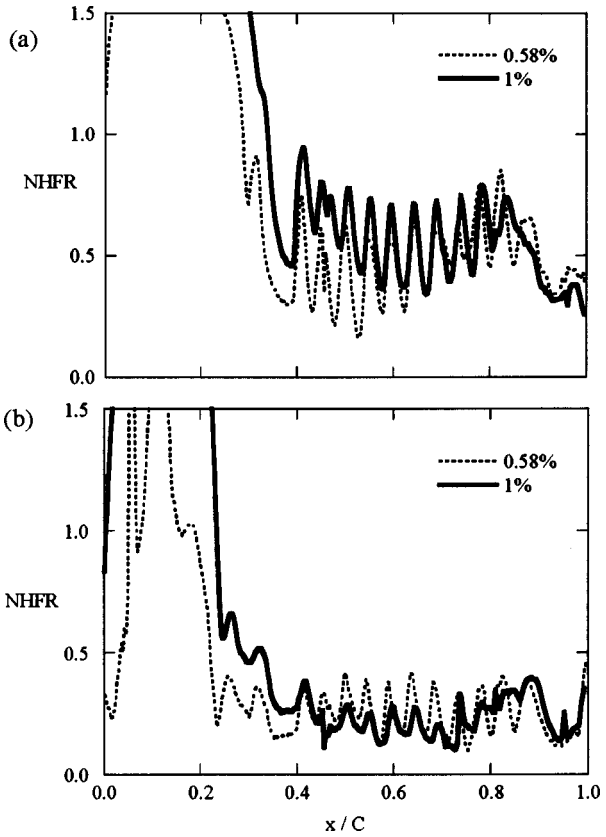

Fig. 15 NHFR levels for camber lines for (*a*) small and (*b*) large tip gap settings

lower blowing ratio than the higher blowing ratio. At the large tip gap (Fig. 15(*b*)) similar trends are seen such that the lower blowing ratio exhibits higher variation between holes than for the higher blowing ratio. Also, increasing the tip gap tends to decrease the NHFR, whereas increased blowing ratio has no noticeable affect on the mean NHFR values.

Area-averaged results of the NHFR are shown in Fig. 16 using both the entire blade tip area and the downstream 70% of the blade tip area. Figure 16 shows increasing NHFR values with increased blowing for the averages over the entire tip surface area. Also, the small tip gap has significantly higher NHFR values than the large tip gap. Because the dirt purge holes dominate the area-averaged results, the NHFR was averaged over the downstream 70% portion of the blade to illustrate the effects blowing and tip gap settings, as shown in Fig. 16. By discounting the dirt purge flow, there is much less dependence on blowing ratio for these results while there is a strong dependence of the tip gap.

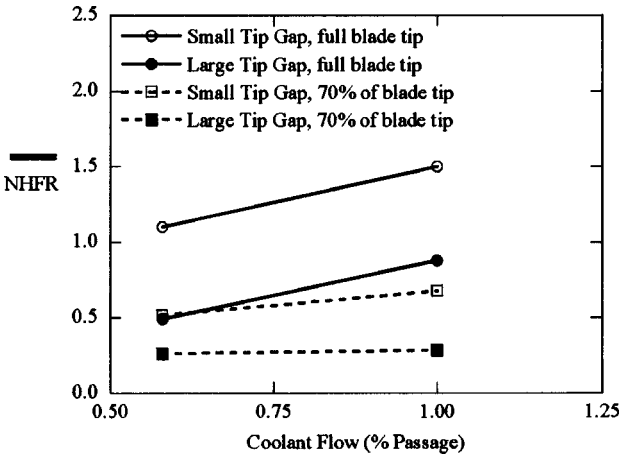

Fig. 16 Area-averaged NHFR for full blade tip and for the downstream 70% of tip

Conclusions

Baseline cases with no blowing at two tip gaps have confirmed that tip heat transfer increases with gap height. This increase can be explained by considering the entry region effect being more dominant for the larger gap distance. Also, a separation region along the pressure side of the tip surface has been indicated by the tip heat transfer measurements. The baseline results showed that there is a small region of low heat transfer, which occurs near the thickest portion of the blade, and tip heat transfer increases toward the trailing edge.

When injecting coolant through pressure-side film-cooling holes, tip heat transfer coefficients are increased above what occurs with no blowing. Increases in the blowing ratio lead to increases in heat transfer on the tip surface. Overall augmentations for the small tip were measured to be larger than for the large tip gap for both blowing ratios.

By evaluating the overall cooling benefit through a net heat flux reduction, the results indicate an overall benefit to the tip by releasing coolant from the pressure-side holes despite increases in the local convective heat transfer coefficients. The area-averaged results for the entire tip indicate relatively little dependence on coolant flow rates and indicate that there is a higher cooling benefit for a small tip gap relative to that of a large tip gap. This higher benefit results from higher adiabatic effectiveness levels.

Acknowledgment

The authors gratefully acknowledge United Technologies–Pratt and Whitney for its support of this work.

Nomenclature

C = true blade chord
D = dirt purge hole diameter
D_h = hydraulic diameter, always used as 2h or 2H
F = augmentation factor for fully developed correlation
h, H = small or large tip gap
h_f = film heat transfer coefficient
h_0 = blade heat transfer coefficient with no blowing
k = thermal conductivity
L = local thickness of blade
$L_{\max}$ = max local thickness of blade
L_T = max thickness of blade overall
NHFR = net heat flux reduction, see Eq. (4)
Nu_{Dh} = Nusselt based on hydraulic diameter, $h(D_h)/k$
Nu_{fd} = Nusselt, fully developed based on hydraulic diameter, $h(D_h)/k$
$\mathrm{Nu}_{0,C}$ = Nusselt based on chord, $h(C)/k$
$\mathrm{Nu}_{0,Dh}$ = Nusselt based on hydraulic diameter, $h(D_h)/k$
Pr = Prandtl number
q''_{tot} = heat flux supplied to tip surface heater
q''_r = heat flux loss due to radiation
R = resistance in Ω.
Re_{in} = Reynolds based on inlet velocity, $U_{in}C/\nu$
Re_{Dh} = Reynolds based on local velocity, $U_{\mathrm{local}}(D_h)/\nu$
$\mathrm{Re}_{ex,Dh}$ = Reynolds based on exit velocity, $U_{ex}(D_h)/\nu$
S = distance from leading edge
$S_{\max}$ = distance from leading to trailing edge
T_w = blade wall temperature
T_∞ = freestream temperature
T_b = background temperature of radiation surface
T_c = coolant temperature
U_{local} = local velocity on tip gap
U_{ex} = exit velocity (at blade trailing edge)

U_{in} = inlet velocity (1 chord upstream)
x = distance along blade chord

Greek

η = film-cooling effectiveness, $(T_{aw}-T_c)/(T_\infty-T_c)$.
ν = fluid dynamic viscosity
ρ = fluid density
ε = emissivity of tip heater surface, always set to 0.93.
θ = dimensionless temperature, $(T_\infty-T_c)/(T_\infty-T_w)$

Superscripts

$=$ = area-averaged value

References

[1] Kwak, J. S., and Han, J. C., 2002, ''Heat Transfer Coefficient on the Squealer Tip and Near Squealer Tip Regions of a Gas Turbine Blade,'' ASME Int. Mech. Eng. Congress and Exposition, ASME Paper No. IMECE 2002-32109.

[2] Christophel, J., Thole, K. A., and Cunha, F., 2005, ''Cooling the Tip of a Turbine Blade Using Pressure Side Holes-Part I: Adiabatic Effectiveness Measurements,'' ASME J. Turbomachinery, **127**, pp. 270–277.

[3] Mayle, R. E., and Metzger, D. E., 1982, ''Heat Transfer at the Tip of an Unshrouded Turbine Blade,'' *Proc. 7th Int. Heat Transfer Conference* **3**, ASME, New York, pp. 87–92.

[4] Morphis, G., and Bindon, J. P., 1988, ''Effect of Relative Motion, Blade Edge Radius and Gap Size on the Blade Tip Pressure Distribution in an Annular Turbine Cascade With Clearance,'' ASME Paper No. 88-GT-256.

[5] Bindon, J. P., 1989, ''The Measurement and Formation of Tip Clearance Loss,'' ASME J. Turbomach., **111**, pp. 257–263.

[6] Bunker, R. S., 2000, ''A Review of Turbine Blade Tip Heat Transfer,'' *Turbine 2000 Symposium on Heat Transfer in Gas Turbine Systems*, Cesme, Turkey.

[7] Bunker, R. S., Bailey, J. C., and Ameri, A. A., 2000, ''Heat Transfer and Flow on the First-Stage Blade Tip of a Power Generation Gas Turbine: Part 1—Experimental Results,'' ASME J. Turbomach., **122**, pp. 263–271.

[8] Jin, P., and Goldstein, R. J., 2003, ''Local Mass/Heat Transfer on a Turbine Blade Tip,'' Int. J. Rotating Mach., **9**(2), pp. 981–995.

[9] Azad, G. S., Han, J. C., and Boyle, R. J., 2000, ''Heat Transfer and Presure Distributions on a Gas Turbine Blade Tip,'' ASME J. Turbomach., **122**, pp. 717–724.

[10] Teng, S., Han, J. C., and Azad, G., 2001, ''Detailed Heat Transfer Coefficient Distributions on a Large-Scale Gas Turbine Blade Tip,'' ASME J. Heat Transfer, **123**, pp. 803–809.

[11] Kwak, J. S., and Han, J. C., 2002, ''Heat Transfer Coefficient and Film-Cooling Effectiveness on a Gas Turbine Blade Tip,'' ASME Turbo Expo, Amsterdam, The Netherlands. Paper No. GT2002-30194.

[12] Saxena, V., Nasir, H., and Ekkad, S. V., 2003, ''Effect of Blade Tip Geometry on Tip Flow and Heat Transfer For a Blade in a Low Speed Cascade,'' ASME Paper No. GT2003-38176.

[13] Ameri, A. A., 2001, ''Heat Transfer and Flow on the Blade Tip of a Gas Turbine Equipped With a Mean-Camberline Strip,'' ASME Paper No. GT2001-0156.

[14] Kim, Y. W., and Metzger, D. E., 1995, ''Heat Transfer and Effectiveness on Film Cooled Turbine Blade Tip Models,'' ASME J. Turbomach., **117**, pp. 12–21.

[15] Kim, Y. W., Downs, J. P., Soechting, F. O., Abdel-Messeh, W., Steuber, G., and Tanrikut, S., 1995, ''A Summary of the Cooled Turbine Blade Tip Heat Transfer and Film Effectiveness Investigations Performed by Dr. D. E. Metzger,'' ASME J. Turbomach., **117**, pp. 1–11.

[16] Hohlfeld, E. M., Christophel, J. R., Couch, E. L., and Thole, K. A., 2003, ''Predictions of Cooling From Dirt Purge Holes Along the Tip of a Turbine Blade,'' ASME Turbo Expo, Atlanta, Georgia. Paper No. GT2003-38251.

[17] Moffat, R. J., 1988, ''Describing the Uncertainties in Experimental Results,'' Exp. Therm. Fluid Sci., **1**, pp. 3–17.

[18] Gnielinski, V., 1976, ''New Equations for Heat and Mass Transfer in Turbulent Pipe and Channel Flow,'' Int. Chem. Eng., **16**, pp. 359–368.

[19] Kakaç, S., Shah, R. K., and Aung, W., 1987, *Handbook of Single-Phase Convective Heat Transfer*, Wiley, New York, pp. 34–35.

[20] Kays, W. M., and Crawford, M. E., 1980, *Convective Heat and Mass Transfer*, Second Edition, McGraw-Hill, New York, pp. 269–270.

[21] Sen, B., Schmidt, D. L., and Bogard, D. G., 1996, ''Film Cooling With Compound Angle Holes: Heat Transfer,'' ASME J. Turbomach., **118**, pp. 800–806.